Rapid hyperspectral, vibrationally resonant sum-frequency generation microscopy

Adam M. Hanninen[a] and Eric O. Potma[b]

[a]Department of Astronomy and Physics, University of California, Irvine, CA 92697, USA
[b]Department of Chemistry, University of California, Irvine, CA 92697, USA

ABSTRACT

We discuss the development and application of a laser-scanning, nonlinear optical microscope capable of generating vibrationally resonant images based on sum-frequency generation (SFG), coherent anti-Stokes Raman scattering (CARS) or third-order sum-frequency generation (TSFG). The combination of these three modalities allows vibrationally sensitive imaging of both $\chi^{(2)}$ and $\chi^{3)}$-active structures in biological tissues, addressing both Raman-active as well as IR-allowed vibrational modes. We show the practical utility of these vibrationally-sensitive modalities by imaging collagen I rich tissues.

Keywords: nonlinear optical microscopy, vibrational spectroscopy

1. INTRODUCTION

Optical microscopy with mid-infrared (MIR; 2.5-10 μm) light enables spectroscopic imaging with contrast based on molecular vibrational modes. Several linear and nonlinear optical imaging techniques with vibrational contrast have been developed for biological applications in the MIR region with high sensitivity. Among these, vibrationally resonant sum-frequency generation (VR-SFG) microscopy is a second-order nonlinear optical imaging technique, which is suitable for imaging biopolymers with a non-vanishing second-order susceptibility $\chi^{(2)}$, such as collagen, microtubules, and cellulose. The molecular modes in VR-SFG are excited with an optical frequency ω_1 in the MIR range, followed by an up-conversion with a second optical frequency ω_2 in the visible/near-infrared range to generate a visible signal at $\omega_1 + \omega_2$, as shown in the Jablonski diagram of Figure 1a. Since $\chi^{(2)}$ is frequency dependent in the MIR range, the signal grows stronger when the ω_1 frequency approaches resonances of SFG-active molecular vibrational modes.

The type of molecular vibrational modes in SFG spectroscopy and microscopy are not necessarily the same modes that are probed in coherent Raman scattering techniques. The transition resonant with ω_1 in SFG is dipole-allowed, whereas the up-conversion step represents a Raman transition. The vibrational modes accessible through the SFG process are thus both IR and Raman-active. The diagram shown in Figure 1b represents the coherent anti-Stokes Raman scattering (CARS) process.[1] Whereas the probing step in both SFG and CARS involves a Raman transition, the preparation step is different. In CARS, the vibrational excitation is Raman-allowed, while in SFG it is dipole-allowed. In addition, CARS is a $\chi^{(3)}$ process, which exhibits different spatial symmetries than the $\chi^{(2)}$ material response. Hence, even though SFG and CARS both probe vibrational transitions, they give rise to complementary contrast in a nonlinear optical (NLO) microscope.[2]

The diagram shown in Figure 1c depicts another vibrational sensitive nonlinear light-matter interaction. This process involves a dipole-allowed ω_1 transition, followed by a two-photon interaction with ω_2 and an instantaneous emission of a photon at $2\omega_2 + \omega_1$. The nonlinear susceptibility of this process is third-order in the field, and thus has the same spatial properties as the CARS process, while the vibrational transition is IR-allowed. The third-order sum-frequency generation (TSFG) signal constitutes another vibrationally-sensitive modality that can be incorporated in the NLO microscope, providing complimentary information to SFG and CARS.

Further author information: (Send correspondence to E.O.P.)
A.H.: E-mail: ahannine@uci.edu
E.O.P.: E-mail: epotma@uci.edu

Multiphoton Microscopy in the Biomedical Sciences XVII, edited by Ammasi Periasamy, Peter T. C. So, Karsten König, Xiaoliang S. Xie, Proc. of SPIE Vol. 10069, 100692H
 · doi: 10.1117/12.2253295

In this presentation, we discuss the construction and application of a microscope capable of generating SFG, CARS and TSFG. The microscope is based on laser scanning a tightly focused spot across the sample with galvanometric mirrors, similar to a conventional NLO microscope, allowing fast image acquisition. Compared to previous versions of the SFG microscope,[3–6] the system presented here is based on a versatile near-infrared, picosecond optical parametric oscillator (OPO). Because the OPO wavelength can be tuned relatively easily, this system enables hyperspectral vibrational imaging based on either of the vibrationally senstive NLO modalities.

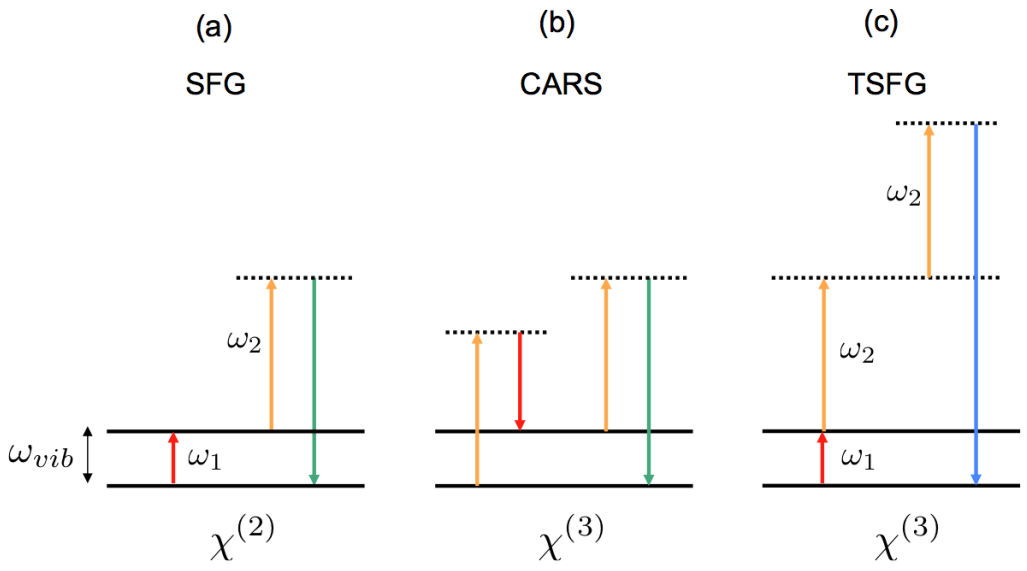

Figure 1. Vibrationally sensitive nonlinear optical light-matter interactions. (a) Sum-frequency generation (SFG). (b) Coherent anti-Stokes Raman scattering (CARS). (c) Third-order sum-frequency generation (TSFG). In this work, all excitation beams are in the NIR or MIR. Specifically, ω_1 is tuned in the 2800 to 3000 cm^{-1} range, whereas ω_2 is fixed at 1030 nm.

2. EXPERIMENTAL

The basic optical layout of the vibrationally sensitive NLO microscope is shown in Figure 2. The main light sources is an Er^+-doped fiber laser centered at 1030 nm (6 ps pulse width, 76 MHz repetition rate) which pumps a synchronously-pumped optical parametric oscillator (Levante OPO, APE Berlin) at a pulse repetition rate of 76-MHz. The OPO is based on a fanned periodically-poled nonlinear crystal, generating a signal in the 1350 nm to 2000 nm range which is resonant in the OPO cavity. The idler beam, which is generated upon each passage of the signal pulse through the crystal, is coupled out and conditioned with a spatial filter. The idler can be tuned from 2200 nm to 4500 nm corresponding to molecular vibrations in the 2220 to 4550 cm^{-1} range. In addition to the signal (NIR) and idler (MIR) delivered by the OPO, the residual pump beam can also be used in the NLO experiments. For SFG, we use the idler beam for the ω_1 excitation, whereas the 1030 nm beam is used for the ω_2 interaction. TSFG is accomplished by using the same outputs from the light source. CARS is achieved by using the 1030 nm beam for the pump interaction and the OPO signal for the Stokes interaction,

The beams are combined on a dichroic mirror in a collinear fashion as shown in Figure 2. The beams subsequently pass through a galvanometric mirror scanning system towards the microscope and focused with a 0.65NA reflective objective onto the sample. The imaging system incorporates CaF_2 scan and tube lenses to enable the use of both NIR and MIR beams. The NLO signals are captured by a refractive condenser lens in the forward direction and passed through a short pass and a bandpass filters before being detected by a photomultiplier tube. In the examples shown here, we focus on the vibrational modes near 2945 cm^{-1}, resulting in a SFG and CARS signal near 790 nm and a TSFG near 445nm.

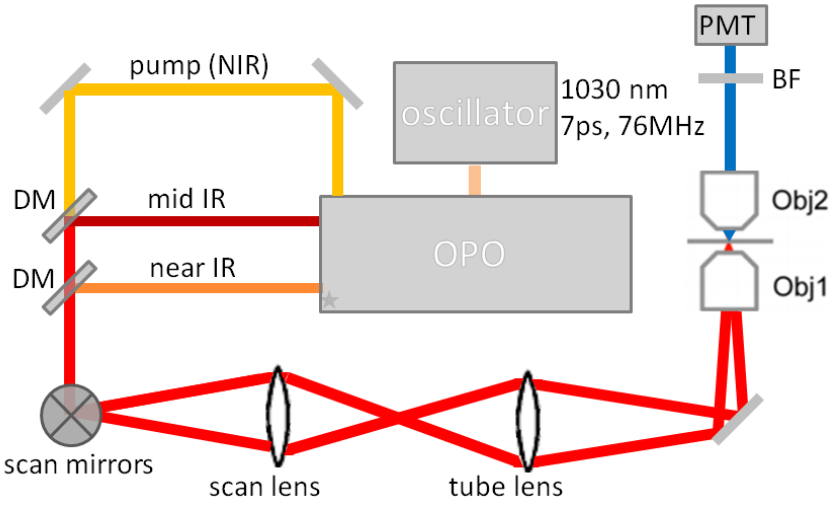

Figure 2. Schematic of the triple-modal vibrational NLO microscope setup. The fiber laser source pumps the OPO to generate a tunable mid-infrared (MIR; idler) beam and a near-infrared (NIR; signal) beam. The point-scanning collinear excitation beams are focused by a microscope objective lens (Obj1) and the signal is collected by a second objective lens (Obj2) in the forward direction. The NLO signals pass through a bandpass filter (BF) and are detected by photomultiplier tubes (PMT).

3. RESULTS

To test the imaging performance and measure the spatial resolution of TSFG we use 0.30 μm diameter barium titanate ($BaTiO_3$) nano-particles as the imaging target. $BaTiO_3$ exhibits a high optical nonlinearity in both second-order $\chi^{(2)}$ and third-order $\chi^{(3)}$ interactions, and therefore produces a strong (non-resonant) nonlinear signal. The SFG image is shown in panel 3a, whereas panel 3b shows the same particles visualized with TSFG contrast. As expected, the $BaTiO_3$ particles are evident in both images. It can be seen that the TSFG image exhibits a slightly higher resolution, due to the higher order nonlinearity of the TSFG process. Both images scale linearly with the MIR beam intensity, but exhibit a different dependence on the ω_2 (1030 nm) beam. The SFG channels depends linearly on the 1030 nm beam intensity, while the TSFG channel shows a quadratic dependence, in accordance with the diagram shown in Figure 1.

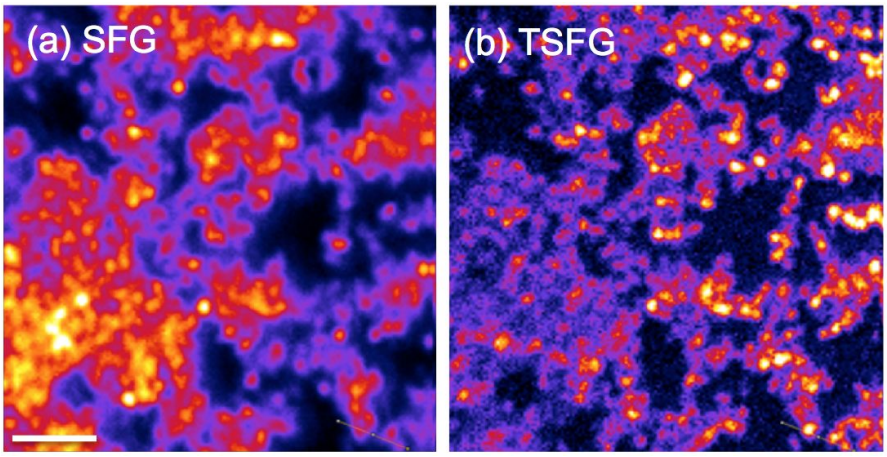

Figure 3. NLO imaging of $BaTiO_3$ nanoparticles on a coverslip. a) SFG signal. b) TSFG signal. The MIR beam (ω_1) is tuned to 2945 cm^{-1} and the NIR beam (ω_2) is fixed at 1030 nm. Scale bar is 5 μm.

In Figure 4, we show an TSFG image obtained from rat tail tendon. This sample is known to show a very strong SFG response,[7,8] but here we are interested in examining the third-order vibrational TSFG response of the sample. For this purpose, the MIR wavelength is tuned to 2945 cm^{-1}, where collagen is known to exhibit a strong C-H stretching vibrational resonance. The image shows the fibrillar collagen structure with clear contrast, indicating that the TSFG modality is capable of generating useful images from biological samples. Note that the TSFG signal contrast is governed not only by vibrational resonance, but also by phase-matching considerations. In this regard, TSFG microscopy shares similarity with third-harmonic generation (THG) microscopy, which is sensitive to nonlinear refractive index changes.[9]

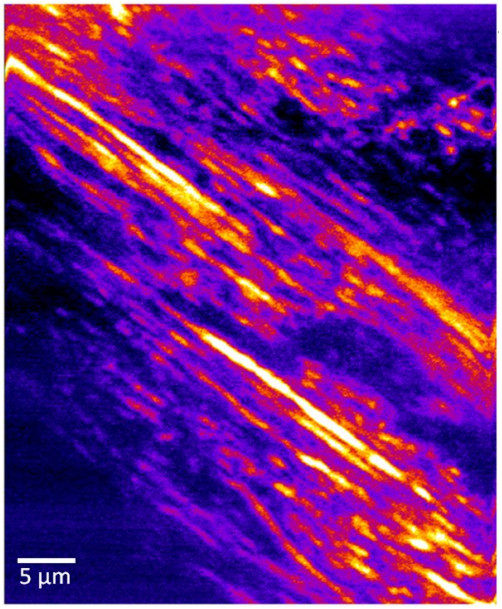

Figure 4. TSFG image of rat tail tendon. The MIR is tuned to the 2945 cm^{-1} C-H stretching vibration of collagen.

Figure 5 shows SFG and CARS images of collagen I fibers in rat tail tendon. The images where acquired form the same area, yet the contrast in the SFG and CARS channels is notably different. When the vibrational resonance is tuned to 2850 cm^{-1}, near the energy of the symmetric CH_2 stretching mode, the CARS image (5c) shows features reminiscent of fibrous structure in the tissue, while the SFG image (5a) exhibits limited contrast. The situation is reversed when the vibrational resonance near 2950 cm^{-1} is examined. For this setting, the SFG image shows bright features (5b), clearly delineating the fibrillar features of collagen. At this vibrational frequency, collagen I shows a strong second-order nonlinearity, which has been attributed to a Fermi-resonance of the methylene-stretching modes[10] of fibrous collagen. The same resonance is not particularly strong in the Raman-sensitive CARS image (5d). This comparison shows that the SFG and CARS channels can provide complementary information.

4. CONCLUSION

In this work, we have demonstrated triple-modal vibrational NLO microscopy, based on SFG, CARS and a new nonlinear optical microscopy modality, TSFG. The combination of these techniques gives access to all Raman-active, IR-active and Raman/IR combination modes, allowing a detailed spectroscopic examination of tissue samples with (sub)-micrometer spatial resolution. Like conventional laser-scanning microscopy, the current imaging platform enables fast scanning, using excitation beams with wavelengths beyond 1 μm. The examples presented here illustrate the capabilities of this imaging system, revealing complementary contrast between the different modalities.

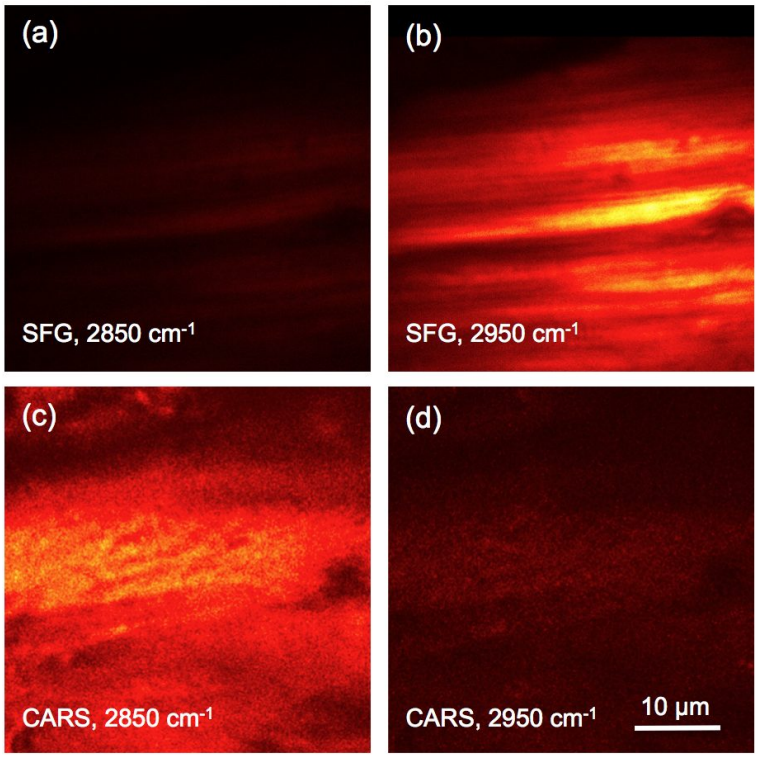

Figure 5. Comparison of SFG and CARS signals from collagen rich tissues. (a) SFG image obtained when ω_1 is tuned to 2850 cm^{-1}. (b) SFG image acquired when $\omega_1 = 2950$ cm^{-1}. (c) CARS image of the same area when the Raman shift is tuned to 2850 cm^{-1}. (d) CARS image when the Raman shift is tuned to 2950 cm^{-1}

ACKNOWLEDGMENTS

We are grateful for funding from the National Science Foundation, grant CHE-1454885, and from the National Institutes of Health, grant P41-RR-01192.

REFERENCES

[1] Cheng, J. X. and Xie, X. S., [*Coherent Raman Scattering Microscopy*], CRC Press, Boca Raton (2013).

[2] Chung, C.-Y., Boik, J., and Potma, E. O., "Biomolecular imaging with coherent nonlinear vibrational microscopy," *Annu. Rev. Phys. Chem.* **64**, 77–99 (2013).

[3] Flörsheimer, M., Brillert, C., and Fuchs, H., "Chemical imaging of interfaces by sum frequency microscopy," *Langmuir* **15**(17), 5437–5439 (1999).

[4] Miyauchi, Y., Sano, H., Okada, J., Yamashita, H., and Mizutani, G., "Simultaneous optical second harmonic and sum frequency intensity image observation of hydrogen deficiency on a H-Si(1 1 1) 1 x 1 surface after IR light pulse irradiation," *Surface Science* **603**(19), 2972–2977 (2009).

[5] Cimatu, K. A. and Baldelli, S., "Chemical microscopy of surfaces by sum frequency generation imaging," *J. Phys. Chem. C* **113**(38), 16575–16588 (2009).

[6] Raghunathan, V., Han, Y., Korth, O., Ge, N.-H., and Potma, E. O., "Rapid vibrational imaging with sum frequency generation microscopy," *Opt. Lett.* **36**(19), 3891–3893 (2011).

[7] Han, Y., Raghunathan, V., Feng, R.-r., Maekawa, H., Chung, C.-Y., Feng, Y., Potma, E. O., and Ge, N.-H., "Mapping molecular orientation with phase sensitive vibrationally resonant sum-frequency generation microscopy," *J. Phys. Chem. B* **117**(20), 6149–6156 (2013).

[8] Han, Y., Hsu, J., Ge, N.-H., and Potma, E. O., "Polarization-sensitive sum-frequency generation microscopy of collagen fibers," *J. Phys. Chem. B* **119**(8), 3356–3365 (2015).

[9] Cheng, J.-X. and Xie, X. S., "Green's function formulation for third-harmonic generation microscopy," *J. Opt. Soc. Am. B* **19**, 1604–1610 (Jul 2002).

[10] Rocha-Mendoza, I., Yankelevich, D. R., Wang, M., Reiser, K. M., Frank, C. W., and Knoesen, A., "Sum frequency vibrational spectroscopy: The molecular origins of the optical second-order nonlinearity of collagen," *Biophysical Journal* **93**, 4433–4444 (2007).